Telomere-based proliferative lifespan barriers in Werner-syndrome fibroblasts involve both p53-dependent and p53-independent mechanisms

Terence Davis[1], Sim K. Singhrao[1], Fiona S. Wyllie[1], Michele F. Haughton[1], Paul J. Smith[1], Marie Wiltshire[1], David Wynford-Thomas[1], Christopher J. Jones[1], Richard G. A. Faragher[2] and David Kipling[1,*]

[1]Department of Pathology, University of Wales College of Medicine, Heath Park, Cardiff, CF14 4XN, UK
[2]School of Pharmacy and Biomolecular Sciences, University of Brighton, Cockcroft Building, Lewes Road, Brighton, BN2 4GJ, UK
*Author for correspondence (e-mail: kiplingd@cardiff.ac.uk)

Accepted 18 December 2002
Journal of Cell Science 116, 1349-1357 © 2003 The Company of Biologists Ltd
doi:10.1242/jcs.00331

Summary

Werner-syndrome fibroblasts have a reduced in vitro life span before entering replicative senescence. Although this has been thought to be causal in the accelerated ageing of this disease, controversy remains as to whether Werner syndrome is showing the acceleration of a normal cellular ageing mechanism or the occurrence of a novel Werner-syndrome-specific process. Here, we analyse the signalling pathways responsible for senescence in Werner-syndrome fibroblasts. Cultured Werner-syndrome (AG05229) fibroblasts senesced after ~20 population doublings with most of the cells having a 2*N* content of DNA. This was associated with hypophosphorylated pRb and high levels of p16^{Ink4a} and p21^{Waf1}. Senescent AG05229 cells re-entered the cell cycle following microinjection of a p53-neutralizing antibody. Similarly, production of the human papilloma virus 16 E6 oncoprotein in presenescent AG05229 cells resulted in senescence being bypassed and extended cellular life span. Werner-syndrome fibroblasts expressing E6 did not proliferate indefinitely but reached a second proliferative lifespan barrier, termed M^{int}, that could be bypassed by forced production of telomerase in post-M1 E6-producing cells. The conclusions from these studies are that: (1) replicative senescence in Werner-syndrome fibroblasts is a telomere-induced p53-dependent event; and (2) the intermediate lifespan barrier M^{int} is also a telomere-induced event, although it appears to be independent of p53. Werner-syndrome fibroblasts resemble normal human fibroblasts for both these proliferative lifespan barriers, with the strong similarity between the signalling pathway linking telomeres to cell-cycle arrest in Werner-syndrome and normal fibroblasts providing further support for the defect in Werner syndrome causing the acceleration of a normal ageing mechanism.

Key words: Ageing, Cellular senescence, Oncoprotein, Microinjection, Telomerase

Introduction

Werner syndrome (WS) is a heavily studied human premature ageing disorder. It is autosomal recessive and characterized by short stature, premature onset of cataracts, skin atrophy and ulceration, hair greying, and age-related diseases such as type-II diabetes mellitus, osteoporosis, soft-tissue calcification and atherosclerosis (Salk, 1982; Epstein et al., 1996; Martin et al., 1999). WS is also associated with an increase in neoplasms of mesenchymal origin (Goto et al., 1996). With the exception of central nervous system degeneration, this disease provides a convincing mimic of the normal ageing phenotype (Brown et al., 1985) and is thus an important model disease.

The underlying genetic defect in WS is a recessive loss-of-function mutation in the *WRN* gene. *WRN* encodes a member of the RecQ helicase family (Yu et al., 1996) which, unlike other members of the RecQ family, also shows 3′ to 5′ exonuclease activity (Huang et al., 1998). WRNp is a nuclear protein that is found predominantly in the nucleoli but that relocates to replication foci at S phase of the cell cycle, and to sites of DNA damage in response to DNA-damaging agents such as 4-nitroquinoline 1-oxide (Gray et al., 1998; Marciniak et al., 1998; Shiratori et al., 1999). It interacts with a range of other proteins, including topoisomerase I, Ku 86/70, replication protein A, p53 and DNA polymerase δ (Shen and Loeb, 2001). WRNp has been implicated in DNA replication, transcription, DNA recombination and DNA repair (Bohr et al., 2002). Although WS cells do show a chromosome instability phenotype (Hoehn et al., 1975; Salk et al., 1981; Fukuchi et al., 1989), WS is not a dramatic DNA-repair-defect syndrome when compared with diseases such as xeroderma pigmentosum. Although WRNp does play a role in DNA repair, loss of expression has only a mild impact on the ability of WS cells to undergo DNA repair (Bohr et al., 2001).

Normal human fibroblasts have a finite capacity to divide, after which they enter a state of permanent cell-cycle arrest termed replicative senescence (also known as mortality stage 1 or M1). Cultures of such cells cease to expand as a result of a progressive decline in the growth fraction. The kinetics of this process have long been recognized to be consistent with the operation of one or more molecular mechanisms capable of acting as a cell division ‘counting’ system. In human dermal fibroblasts, it is now known that this counting mechanism is based on the activation of p53 as a result of the progressive erosion of chromosomal telomeres (Bodnar et al., 1998; Vaziri and Benchimol, 1998; Wright and Shay, 2002).

WS fibroblast cultures display a dramatic reduction in replicative life span (Martin et al., 1970) owing to an increased rate of decline in the culture growth fraction compared with normal controls (Faragher et al., 1993). Loss of the WRN helicase has the potential to produce many abortive DNA replication events that could trigger premature cell-cycle exit without involving telomeric loss. Thus, an important but unresolved question is the extent to which the rapid replicative senescence seen in WS fibroblasts results from an acceleration of normal senescence mechanisms and to what extent (if any) it results from chromosomal instability and replication-fork stalling as a result of mutations in *WRN*.

Although several groups have shown that telomere shortening acts as a primary driver of senescence in WS fibroblasts (Ouellette et al., 2000; Wyllie et al., 2000; Choi et al., 2001), these studies did not address in detail the signalling pathway downstream of telomere erosion in WS cells. Replicative senescence is associated, in the case of dermal fibroblasts from newborns or adults, with activation of p53 as a transcriptional transactivator (Itahana et al., 2001), as shown by the induction of p53-dependent transcripts such as the cyclin-dependent kinase inhibitor p21^{Waf1} or p53-dependent reporter constructs in senescent fibroblasts (Bond et al., 1994; Bond et al.,1995; Bond et al., 1996; Webley et al., 2000). Furthermore, abrogation of p53 function using dominant-negative p53 alleles, microinjection of anti-p53 antibodies or viral oncoproteins such as human papilloma virus 16 (HPV16) E6 leads to a bypassing of senescence and extension of lifespan (Bond et al., 1994; Bond et al., 1999; Gire and Wynford-Thomas, 1998).

Accordingly, in the present study, we address whether replicative senescence in WS fibroblasts shows features consistent with an acceleration of the mechanism of senescence that is seen in normal dermal fibroblasts. Two complementary experimental approaches were undertaken: (1) observational studies of key cell-cycle proteins (including those normally involved in the p53 response); and (2) direct experimental abrogation of p53 function using two independent methods.

Materials and Methods

Cell culture

HCA2 human diploid fibroblasts were provided by Jim Smith (Baylor College of Medicine, Houston, Texas). WS cell strain AG05229 was obtained from the Coriell NIA Aging Cell Culture Repository (Camden, New Jersey). All cells were grown in Dulbecco's modified Eagle medium (Life Technologies) supplemented with 10% foetal calf serum (Imperial Labs). Determination of in vitro life span and passage protocols were as described by Bond et al. (Bond et al., 1996).

Retroviral gene transfer

Amphotropic retrovirus vectors expressing the HPV16 E6 oncoprotein from a pLXSN construct, packaged in PA317 cells (Halbert et al., 1991), were kindly provided by Denise Galloway (University of Washington, Seattle, WA). pBABEhTERT (Wyllie et al., 2000) is an amphotropic retrovirus expressing hTERT, the catalytic protein subunit of human telomerase, constructed by cloning the *Eco*RI insert of pGRN121 (Nakamura et al., 1997) into pBABEpuro (Morgenstern and Land, 1990). For control infections, pBABEneo, or pBABEpuro vectors, packaged in ψCRIP cells, were used (Wyllie et al., 2000).

Gene transfer was carried out as described previously (Bond et al., 1994). Two days later, fibroblast cultures were passed into medium containing G418 (0.4 mg ml^{-1}), or puromycin (2.5 μg ml^{-1}), at serial dilutions of 1:5, 1:10, 1:100 and 1:250, and observed for colony development. For each gene transfer, the retroviral infections were done twice.

BrdU incorporation assays

Cells were labelled by incubation in 10 μM bromodeoxyuridine (BrdU) for 1 hour, with incorporation detected by immunoperoxidase (Bond et al., 1996). The proportion of BrdU-positive cells was assessed in a total count of 500 cells.

Detection of senescence-associated β-galactosidase activity

Endogenous mammalian senescence-associated β-galactosidase activity (SAβ-gal) was assessed histochemically (Dimri et al., 1996; Bond et al., 1999). The proportion of β-galactosidase-positive cells was assessed in a total count of 500 cells.

Apoptosis (TUNEL) assays

Cytospin preparations of trypsinized cultures were prepared, treated and incubated with terminal deoxynucleotidyl transferase (Promega) and biotin-16-dUTP (Boehringer Mannheim) as described in (Bond et al., 1999). Sites of biotin-16-dUTP localization were visualized by using the mouse-specific avidin-biotin-peroxidase (ABC) system (Vector Labs) (Bond et al., 1999). After haematoxylin counterstaining, the proportion of apoptotic (brown) cells was assessed in samples of 500 cells.

Immunocytochemistry

For p21^{Waf1}, cells on coverslips were fixed and pre-treated as described (Bond et al., 1999). p21^{Waf1} was detected by incubation for 1 hour in a 1:500 dilution of an anti-p21^{Waf1} mouse monoclonal antibody (6B6; Becton Dickinson), followed by a 1:100 dilution of biotinylated anti-mouse antibodies using the ABC kit (Vector Labs). The proportion of p21^{Waf1}-positive cells was assessed in a total count of 500 cells.

Immunoblotting

Protein samples were prepared, separated on 12% sodium-dodecyl-sulphate/polyacrylamide electrophoresis gels (for pRb, a 7.5% gel was used), electroblotted to Immobilon-P polyvinylidene difluoride membrane (Millipore) and antibodies applied as described by Bond et al. (Bond et al., 1999). The antibodies used were: mouse monoclonal anti-p21^{Waf1} (6B6; Becton Dickinson); mouse monoclonal anti-p16^{Ink4a} (DCS50; Oncogene Research Products); mouse monoclonal anti-p27^{Kip1} (C20; Transduction Laboratories); mouse monoclonal anti-p53 (DO-1; Calbiochem); mouse anti-pRb (C3-245; Becton Dickinson). A chemiluminescence kit (Amersham) was used for visualization using goat anti-mouse secondary antibodies. After visualization, blots were washed three times for 10 minutes in 0.1 M glycine (pH 2.5), once in 1 M Tris (pH 8.0) for 5 minutes, and then in PBS for 30 minutes, before reuse. After use, the filter was stained with India ink.

Densitometric quantification analysis

Quantification of the specific signal and the amount of protein loaded for the immunoblot (Fig. 2) was performed using a Bio-Rad imaging densitometer with Molecular Analyst software. When normalized based on protein loading, the relative amounts of p21^{Waf1} are 1.0 and 1.17 (arbitrary units) for cycling WS cells and WS cells at M1,

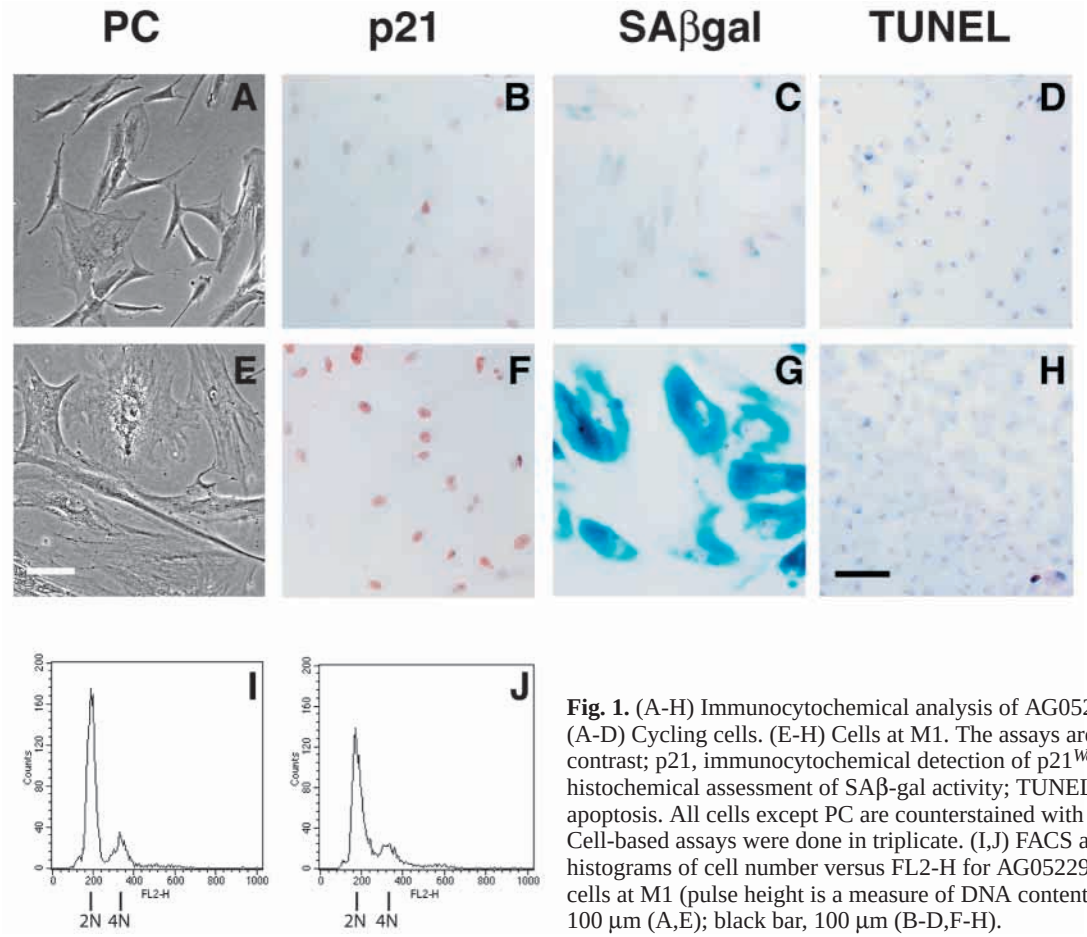

Fig. 1. (A-H) Immunocytochemical analysis of AG05229 cells. (A-D) Cycling cells. (E-H) Cells at M1. The assays are: PC, phase contrast; p21, immunocytochemical detection of $p21^{Waf1}$; SAβgal, histochemical assessment of SAβ-gal activity; TUNEL, assay for apoptosis. All cells except PC are counterstained with haematoxylin. Cell-based assays were done in triplicate. (I,J) FACS analysis histograms of cell number versus FL2-H for AG05229 and HCA2 cells at M1 (pulse height is a measure of DNA content). White bar, 100 μm (A,E); black bar, 100 μm (B-D,F-H).

respectively. WS cells at M1 have ~2.4 times more total protein per cell than cycling WS cells (not shown), a figure similar to that seen for IMR90 cells (Sherwood et al., 1988). Thus, taking into account both the higher relative amount of $p21^{Waf1}$ determined from Fig. 2 (1.17 times) and the increased amount of total protein per cell (2.4 times), WS cells at M1 have ~2.7 times as much $p21^{Waf1}$ per cell than cycling WS cells.

Microinjection of anti-p53 antibodies

Late-passage AG05229 cells were microinjected using an Eppendorf system as described previously (Bond et al., 1996). Mouse monoclonal antibody DO-1 (isotype $IgG_{2a}\kappa$; Oncogene Research) or control mouse IgG (Sigma) was injected at a concentration of 2 mg ml^{-1} in PBS. Rabbit IgG (12 mg ml^{-1}) (Sigma) was co-injected. Following injection, cells were incubated in fresh medium for 48 hours and then incubated in 20 μM BrdU for 4 hours. Cells were fixed as described above and BrdU incorporation was detected by incubation in a 1:100 dilution of anti-BrdU (isotype $IgG_1\kappa$) (Dako) with DNAase I (25 U ml^{-1}) for 2 hours at 37°C, followed by incubation for 1 hour at room temperature in a 1:50 dilution of fluorescein isothiocyanate (FITC) conjugated goat anti-mouse IgG_1-isotype specific (Southern Biotechnology Associates). The isotype-specific FITC-IgG_1 is used to avoid a cross-reaction with microinjected DO-1. Microinjected cells were detected using a 1:800 dilution of goat anti-rabbit-Texas Red conjugate (Southern Biotechnology Associates). Nuclei were visualized by staining with 0.5 μg ml^{-1} 4′-6-diamidino-2-phenylindole (DAPI) for 5 minutes at room temperature, and the cells were mounted in 90% glycerol-PBS. All antibody dilutions were in 1% bovine serum albumin in PBS.

Cell-cycle analysis

Cells were washed twice with PBS prior to trypsinization. All cell-culture media and PBS washes were collected with trypsinized cells and spun down for 10 minutes at 300 ***g***. Cell pellets were adjusted to 1 ml (3-6×10^5 cells ml^{-1}). 125 μl of 0.4 mg ml^{-1} ethidium bromide and 1% Triton X-100 was added, followed by 50 μl ribonuclease A (10 mg ml^{-1}). Samples were vortexed, incubated at room temperature for 10 minutes and then immediately analysed by flow cytometry (Smith et al., 1999). Direct observation of cell suspensions indicated minimal doublet formation. Cell samples were analysed using a FACScan flow cytometer (Becton Dickinson Immunocytometry Systems). Histograms of cell numbers versus FL2-H (pulse height) provided a measure of the DNA content of the cells.

Results

Growth characteristics of WS AG05229 fibroblasts

WS AG05229 fibroblasts at a population-doubling (PD) level of 12 were passaged every 3-4 days until the cells entered replicative senescence (M1), indicated by accumulation of cells with a large irregular morphology (Fig. 1E), a BrdU labelling index (LI) of 1.8±0.6%, a high level of SAβ-gal activity (95±1%) (Fig. 1G) and a low rate of cell death (<1%) as determined by TUNEL assay (Fig. 1H). At this point, the cells had undergone a total of 20.5 PDs since explantation, so AG05229 has the reduced replicative potential reported for these cells (Choi et al., 2001) that is typical of WS fibroblasts in culture (Martin et al., 1970; Faragher et al., 1993).

Most of the AG05229 cells at M1 (>77%) were arrested

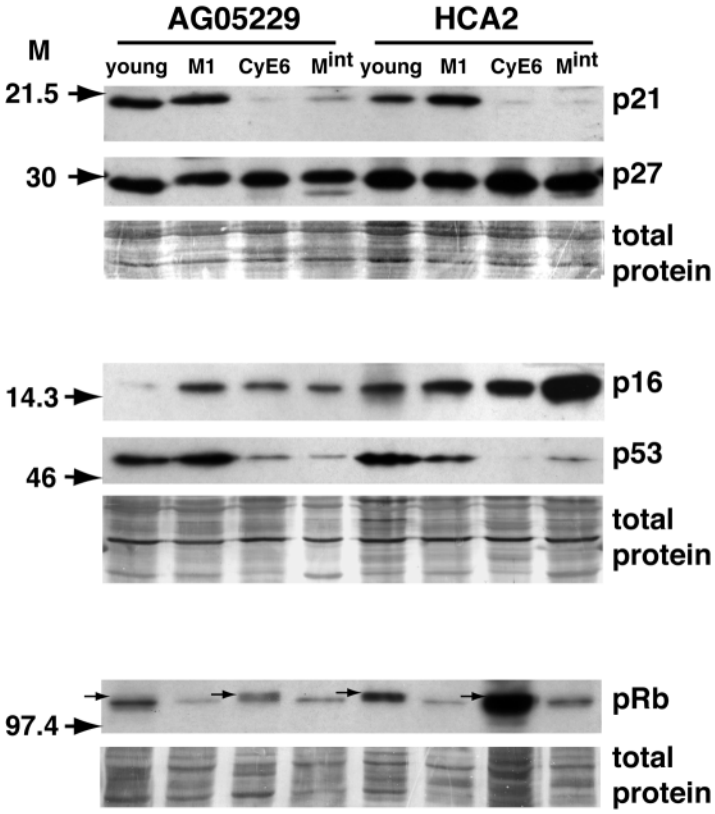

Fig. 2. Immunoblot analysis of AG05229 and HCA2 fibroblasts with or without the expression of HPV16 E6. Lysates were prepared from cycling cells (young), senescent cells (M1), cycling E6-infected cells (CyE6) and E6-infected cells at M^{int} (M^{int}) for both AG05229 and HCA2. Expression levels were compared for various cell-cycle components as indicated. Approximately equal amounts of cell lysate protein (23 μg top, 19 μg middle and 11 μg bottom panels, respectively) were loaded per lane as verified by India-ink staining; the HCA2 cells at CyE6 lane in the bottom panel is slightly overloaded. Molecular mass markers (M) are shown in kDa. The hyperphosphorylated forms of pRb are denoted by the small arrows.

with a 2*N* DNA content as assessed by fluorescence-activated cell sorting (FACS) analysis (Fig. 1I), which is consistent with G_1 arrest. However, a significant proportion (~20%) had higher levels, reflecting G_2 arrest and/or G_1 tetraploid cells. The same overall pattern was seen with control HCA2 cells (Fig. 1J) and has been reported for IMR90 cells (Sherwood et al., 1988).

Cycling AG05229 cells showed moderate levels of the cyclin-dependent kinase inhibitor (CdkI) $p21^{Waf1}$ in 22.5±1.8% of the nuclei by immunocytochemistry (Fig. 1B). This increased to 91.2±1.3% of the nuclei by the time the cells reached M1 (Fig. 1F). Although, when analysed by immunoblot using anti-$p21^{Waf1}$ antibodies, cycling and M1 AG05229 cells appeared to have similar levels of $p21^{Waf1}$ (Fig. 2), once quantified on a per-cell basis (see Materials and Methods) to take into account the observation that cells at M1 have approximately twice the protein of cycling cells (Sherwood et al., 1988), it is clear that there has been a significant increase in the level of $p21^{Waf1}$ as WS cells reach M1. The presence of cycling cells in the young AG05229 population was indicated by their small size (Fig. 1A), a BrdU LI of 29.5±2%, low levels of SAβ-gal activity (6±1.1%) (Fig. 1C) and the presence of low but detectable levels of hyperphosphorylated pRb (Fig. 2).

We have also examined the levels of two other CdkIs in AG05229 cells. The CdkI $p16^{Ink4a}$ was present at almost undetectable levels in cycling AG05229 cells (Fig. 2) and showed a large increase as these cells reached M1. By contrast, there was no significant difference in the level of the $p21^{Waf1}$-related CdkI $p27^{Kip1}$ as the AG05229 cells reached M1 (Fig. 2). The same overall pattern of expression of these CdkIs is seen in HCA2 cells as they proceed to M1 (Fig. 2).

Abrogation of p53 function extends the cellular life span of WS fibroblasts

Presenescent AG05229 fibroblasts at 20 PDs (BrdU LI of 3.4±0.8%) were infected with amphotropic retroviral vectors encoding a neomycin resistance gene (neo^R) alone (Wyllie et al., 1993) or with HPV16 E6 (Halbert et al., 1991). Analysis of G418-resistant colonies (designated 5229.neo and 5229.E6) began two to three weeks after infection.

As expected, cells expressing neo^R alone ceased proliferating during the first two weeks and entered replicative senescence, forming clones of up to 5 PDs (32 cells) (Fig. 3B). The 5229.neo cells at this stage were essentially identical to uninfected AG05229 cells at M1 (not shown). By contrast, expression of HPV16 E6 resulted in evasion of senescence and generated rapidly growing colonies as observed visually (Fig. 3, Fig. 4A). As the 5229.E6 colonies grew, they consistently went through a brief phase of cell death coupled with continued colony expansion

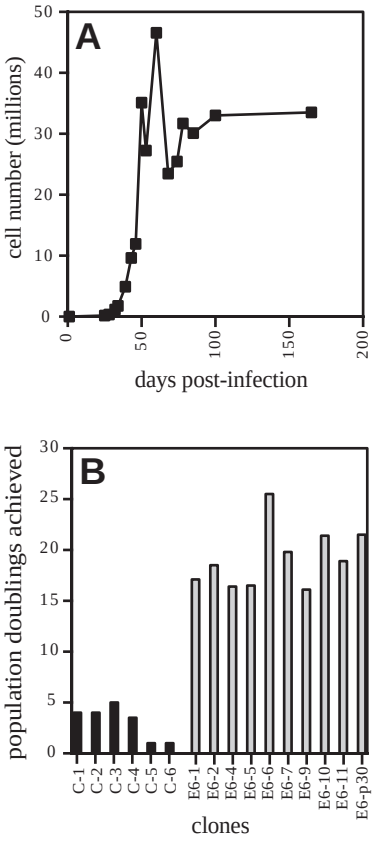

Fig. 3. Extension of cellular lifespan of Werner-syndrome fibroblasts following abrogation of p53 function by HPV E6. (A) Growth curve of total cell number versus time for E6-infected AG05229 clone 6. (B) Comparison of growth levels achieved for control (C-1 to C-6) and E6-infected (E6-1 to E6-11) AG05229 clones. E6-p30 is a pooled sample of 30 G418-resistant colonies.

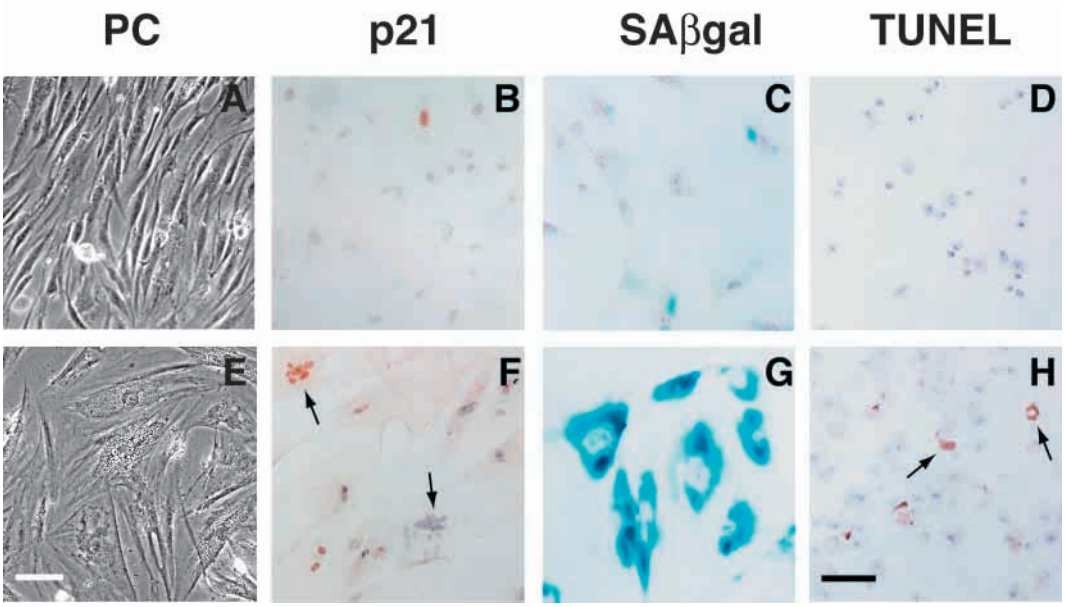

Fig. 4. Immunocytochemical analysis of E6-expressing AG05229 cells. (A-D) Cycling E6-infected cells. (E-H) E6-infected cells at M^{int}. The assays are: PC, phase contrast; p21, immunocytochemical detection of $p21^{Waf1}$; SAβgal, histochemical assessment of SAβ-gal activity; TUNEL, assay for apoptosis. Arrows indicate multinucleate cells (F) and apoptotic cells (H). All cells except PC are counterstained with haematoxylin. Cell-based assays were done in triplicate. White bar, 100 μm (A,E); black bar, 100 μm (B-D,F-H).

(Fig. 3A). Eventually, >80 days post-infection, net growth ceased and the cells entered a state similar to the second senescence-like state, which we have termed M^{int} in HCA2.E6 fibroblasts (Bond et al., 1999). The presence of cell death makes the absolute determination of lifespan extension in the 5229.E6 colonies problematical. However, the M^{int}-like state was reached with a final cell count equivalent to 15-25 PDs post-infection (10-20 PDs beyond M1; Fig. 3B). A pooled sample of 30 colonies (5229.E6p30) arrested in a M^{int}-like state after 21.5 PDs post-infection (Fig. 3B), but a crisis-like phase was not obvious, possibly owing to the mixed population of clones of differing lifespans.

The young 5229.E6 cells (<13 PDs post-infection) were small (Fig. 4A), showed a high BrdU LI (25.2±1.8%), a low SAβ-gal index (3.5±0.8%) (Fig. 4C) and a TUNEL index of <1%, indicating that there was no significant cell death occurring (Fig. 4D).

The WS cells at M^{int} were very large and highly irregular in morphology (Fig. 4E), with a low BrdU LI (1.8±0.6%) and a high SAβ-gal index (92.6±1.2%) (Fig. 4G). FACS analysis showed a significant proportion (~8%) of M^{int} cells with >4*N* DNA content, indicating the presence of polyploid cells (not shown). An inspection of 5229.E6 cells fixed on coverslips revealed that 9±1.3% of the M^{int} cells had more than two nuclei (Fig. 4F). Lower-power inspection of the culture revealed a low, but significant, level of phase-bright cells that probably represent mitoses (not shown), and there was a build up of cell debris in the culture medium, suggesting the occurrence of cell death. TUNEL analysis showed 5±1.0% positive nuclei (Fig. 4H), suggesting that some of this cell death was due to apoptosis. However, overall cell number was stable (with occasional refeeding) in this state for several weeks.

Expression of cell-cycle proteins in normal and WS fibroblasts

Cycling AG05229 cells showed moderate levels of $p21^{Waf1}$ in 22.5%±1.8% of the nuclei by immunocytochemistry, which increased to 91.2%±1.3% of the nuclei by the time the cells reached M1. Expression of HPV16 E6 caused a dramatic decrease in both the intensity and proportion of nuclei positive for $p21^{Waf1}$, with only 2.5±0.7% of nuclei showing detectable immunostaining at 20 days (Fig. 4B). The cells at this time had undergone ~13 PDs since infection and were growing rapidly. This was followed by a slow increase in the number of immunopositive nuclei, reaching 15±1.6% by M^{int} (Fig. 4F).

Immunoblot analysis using anti-$p21^{Waf1}$ antibodies confirmed the immunocytochemistry data (Fig. 2). (The reasons for the apparently similar levels of $p21^{Waf1}$ protein in cycling and M1 AG05229 cells are outlined above.) In control HCA2 fibroblasts, the level of $p21^{Waf1}$ was low in cycling cells and high in senescent cells (Fig. 2). When E6 was introduced into the cells, the level of $p21^{Waf1}$ was reduced to almost undetectable levels, although they rose slightly as the cells entered the M^{int}, for both 5229.E6 and HCA2.E6 cells (Fig. 2).

p53 was readily detectable in AG05229 and HCA2 cells in both cycling cells and at M1 (Fig. 2). In the E6-infected cells, however, p53 protein was barely detectable, confirming E6-mediated degradation of p53 (Fig. 2). These data, taken together, indicate that $p21^{Waf1}$ is upregulated at M1 and that abrogation of p53 using E6 results in a low level of expression of $p21^{Waf1}$ for both AG05229 and HCA2 cells.

The level of the CdkI $p16^{Ink4a}$ is reported to increase in HCA2 cells when they reach M1 (Bond et al., 1999). This increases further in E6-infected HCA2 cells as they reach M^{int} (Bond et al., 1999) (Fig. 2), suggesting that increased $p16^{Ink4a}$ production might compensate for the lack of $p21^{Waf1}$ production in cell-cycle arrest. An increase in $p16^{Ink4a}$ was seen in WS cells as they reached M1, but no further increase was found as 5229.E6 cells reached M^{int} (Fig. 2). Densitometric analysis indicated that the low level of $p16^{Ink4a}$ seen at M^{int} was not due to different protein loading. In fact, the level of $p16^{Ink4a}$ might actually have decreased in these cells after E6 production, although the level increased again as the cells reached M^{int} without reaching the level seen at M1.

The CdkI $p27^{Kip1}$ has been reported to be elevated in senescent human fibroblasts (Bringold and Serrano, 2000). Thus we probed the western blot with anti-$p27^{Kip1}$ antibodies

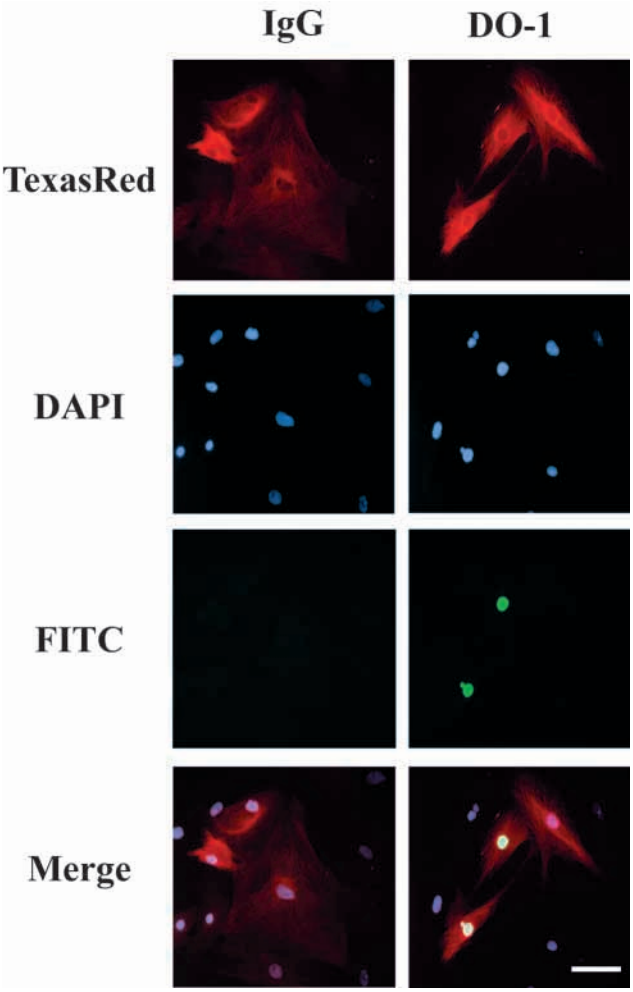

Fig. 5. Microinjection of control IgG or anti-p53 antibodies into senescent AG05229 cells. The injected cells are marked by Texas Red, nuclei are detected by DAPI staining and BrdU incorporation is marked by FITC. The images are merged in the bottom panels. The DO-1-injected cells show two nuclei incorporating BrdU. Bar, 100 μm.

and found no obvious changes in the levels of $p27^{Kip1}$ in any of the WS or HCA2 samples in this study (Fig. 2).

The presence of cycling cells in some of these populations was indicated by probing the western blots with an anti-pRb antibody that detects both hyper- and hypophosphorylated forms of pRb; the hypophosphorylated form of pRb is growth inhibitory (Stein et al., 1990). In all the cycling populations, a doublet was detected (indicated by the arrows), which was not seen in any of the four noncycling populations (Fig. 2). As noted above, the upper hyperphosphorylated band was present at a reduced level in cycling WS cells.

Senescent WS fibroblasts undergo DNA synthesis after injection of a p53-neutralizing antibody

The lifespan extension of WS cells following production of HPV16 E6 is consistent with a p53-dependent cell-cycle arrest. However, because of the many non-p53 targets of E6, we wished to provide an independent method of abrogating p53 function in WS AG05229 cells. The anti-p53 antibody DO-1 recognizes an epitope within the N terminus of p53 (amino acids 20-25) (Stephen et al., 1995; Böttger et al., 1996) that includes key residues required for transactivation (amino acids 22 and 23) (Lin et al., 1995). Previous work has shown that microinjection of DO-1 antibodies into senescent HCA2 cells effectively abrogates p53 activity and allows the cells to re-enter the cell cycle (Gire and Wynford-Thomas, 1998).

Thus, DO-1 antibodies were introduced by microinjection into senescent AG05229 cells (BrdU LI of 1.8±0.6%). 48 hours after injection, 13/68 (19.1±4%) of the DO-1-injected cells were synthesising DNA as assessed by a 4-hour BrdU pulse, compared with 0/30 (0%) of cells injected with the control antibodies (Fig. 5). Thus, antibody abrogation of p53 function results in these cells re-entering the cell cycle and provides confirmation that M1 arrest in WS cells is a p53-dependent process.

Spontaneous escape from M^{int} in WS fibroblasts

Pooled 5229.E6p30 cells at M^{int} were maintained with regular refeeding for several weeks without net gain or loss in cell number (Fig. 6A). They had a low BrdU LI (1.8±0.6%) and a high SAβ-gal index (>90%) throughout this period of stationary growth (not shown). Visual inspection revealed a low level of mitotic cells (Fig. 6B), that most cells had a large, irregular morphology and that there was a gradual build up of cellular debris.

Interestingly, however, ~150 days after the onset of the M^{int}-like state (257 days post-infection), the culture began to expand rapidly (Fig. 6A). Most cells at this time were small with similar morphology to uninfected growing cells, although there was a significant proportion of M^{int}-like cells and many mitoses were present (Fig. 6C). The cells had a high BrdU LI (39.6±2.2%) and a low SAβ-gal index (2.2±0.65%) at a PD level of 26.2 (i.e. ~5 PDs beyond the M^{int}-like state) (not shown). After more than 280 days post-infection, the population began to decrease in total cell number, coincident with a marked increase in the levels of cell death. This behaviour resembled a crisis state, with the cells having an apoptotic index of 5±1% as assayed by TUNEL analysis (not shown). The cells at this stage were very irregular in morphology and apoptotic-like cells could be seen clearly (Fig. 6D). After 410 days post-infection, all the cells of the 5229.E6p30 culture had died.

M^{int} in WS fibroblasts is a telomere-dependent, p53-independent event

WS fibroblasts can bypass the M1 senescent state and be immortalized by the ectopic production of the human telomerase catalytic subunit hTERT (Ouellette et al., 2000; Wyllie et al., 2000), indicating that M1 is telomere driven. To investigate whether M^{int} is also a telomere-driven event, we produced telomerase in post-M1 5229.E6 cells. Late-passage 5229.E6 cells were infected with amphotropic viruses expressing either the puromycin resistance gene alone or the puromycin resistance and hTERT genes. The cells used were 5229.E6 clone 6 at a PD level of 20.5 (post-infection), which are beyond M1 but still distant from M^{int}, which occurs at ~25 PDs in this clone.

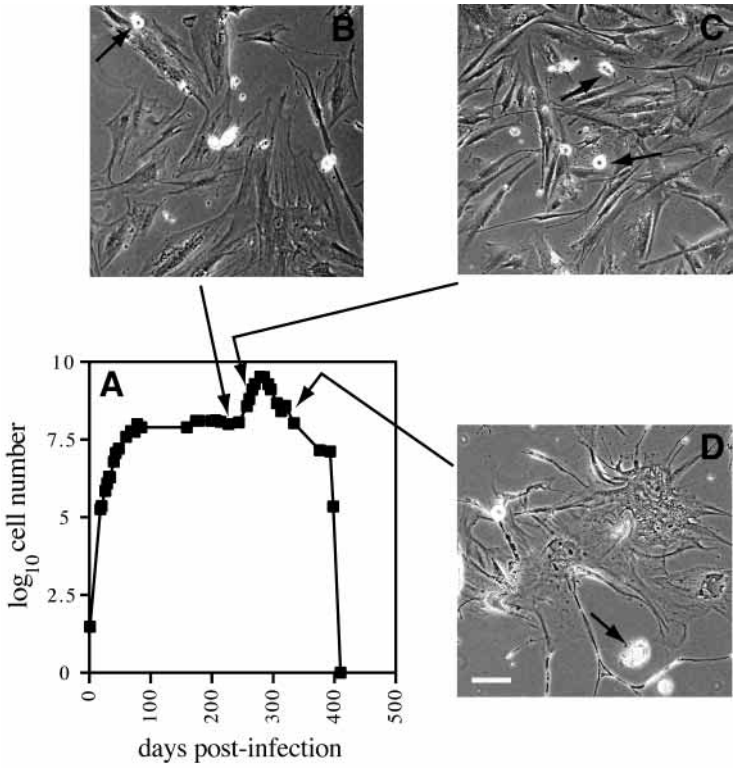

Fig. 6. Growth characteristics of 5229.E6p30 cells that escape M^{int}. (A) Growth kinetics. (B-D) Phase contrast images showing the cells at 250 days (B), 270 days (C) and 350 days (D) post-infection. Arrows indicate mitotic cells (B,C) and apoptotic-like cells (D). Bar, 100 μm.

Analysis of puromycin-resistant colonies (designated 5229.E6.puro and 5229.E6.hTERT) was begun 4-5 weeks after infection. The 5229.E6.puro clones reached a stationary phase resembling M^{int} after 49 days (BrdU LI of 3.8±0.85% and SAβ-gal index of 91±1.3%) at ~9 PDs post-infection, and no expansion in cell numbers was seen over a further 56 days (Fig. 7A,B). Conversely, both of the two 5229.E6.hTERT clones continued expanding and have now reached a total of 33 and 44 PDs post-infection and are still growing (Fig. 7A,B). These cells were small (Fig. 7C) and had growth characteristics similar to young AG05229 cells (BrdU LI of 23.4±1.9%, $p21^{Waf1}$ labelling of 1.6±0.6%, SAβ-gal index of 3.4±0.8%, TUNEL level of <1%; data not shown). Thus, it appears that ectopic expression of hTERT is sufficient for post-M1 E6-infected AG05229 fibroblasts to avoid M^{int}, suggesting that M^{int} is a p53-independent proliferative lifespan barrier that requires telomere erosion.

Discussion

WS AG05229 fibroblasts in culture undergo senescence after a reduced replicative lifespan compared with normal dermal fibroblasts. At M1, most cells (>77%) have a 2*N* DNA content, suggestive of a G_1-S arrest, but a significant proportion (~20%) have a higher DNA content indicative of either G_1 tetraploid cells or G_2-M arrest. The presence of significant numbers of G_1 tetraploid cells at M1 has been reported for IMR90 cells by karyotype analysis of metaphase cells (Sherwood et al., 1988), suggesting that AG05229 cells with a G_2-M DNA content are also G_1 tetraploids. WS cells at M1 resemble senescent normal cells in morphology, BrdU LI, SAβ-gal activity and a low level of cell death (Bond et al., 1999; Dulic et al., 2000). Similarly, they have elevated levels of the Cdk inhibitors $p21^{Waf1}$ and $p16^{Ink4a}$, and abrogation of p53 by microinjection of anti-p53 antibodies into senescent cells allowed them to re-enter the cell cycle. These data, together with the observation that ectopic expression of telomerase allows WS cells to avoid M1 (Ouellette et al., 2000; Wyllie et al., 2000; Choi et al., 2001), are consistent with senescence in WS cells being a telomere-driven p53-dependent event, and suggest that M1 in WS cells is essentially identical to M1 in normal fibroblasts (Gire and Wynford-Thomas, 1998; Bond et al., 1999; Dulic et al., 2000).

Expression of HPV16 E6 causes WS cells to bypass M1 and to continue growth until reaching a second proliferative lifespan barrier, M^{int}, after a similar number of PDs to HCA2.E6 cells (Bond et al., 1999). Most WS.E6 cells at M^{int} resemble normal M^{int} fibroblasts in that they are very large and have a low level of BrdU incorporation and high SAβ-gal activity. In E6-infected WS cells, the level of $p21^{Waf1}$ is much

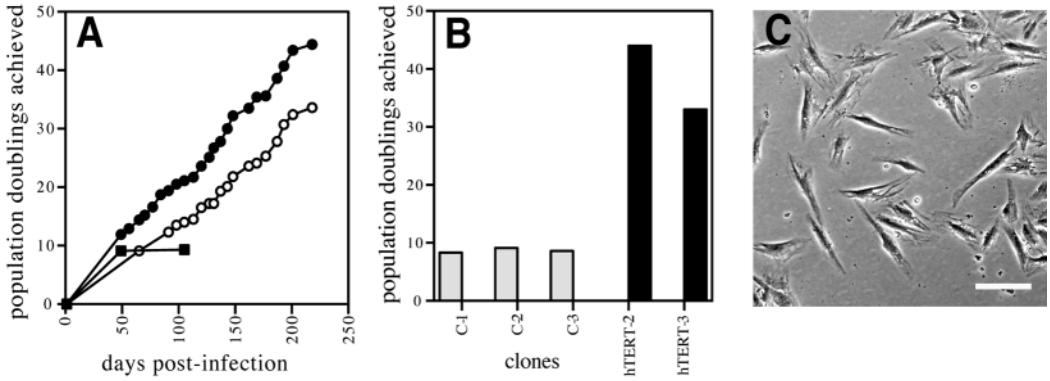

Fig. 7. Growth characteristics of 5229.E6 cells infected with hTERT. (A) Growth curve of population doublings achieved against time: ●, E6.hTERT clone 2; ○, E6.hTERT clone 3; ■, growth of the control clones (only clone 2 shown for clarity). (B) The same data as represented by a histogram. C-1 to C-3 are the control clones and hTERT-1 and hTERT-2 are the hTERT-infected clones. (C) Phase-contrast image showing the morphology of the E6.hTERT cells. Bar, 100 μm.

reduced and only rises slightly as the cells reach M^{int}. Similar changes in $p21^{Waf1}$ are also seen in HCA2.E6 and IMR90.E6 cells (Bond et al., 1999; Dulic et al., 2000). This is correlated with the reduced levels of p53 found in these cells. Together with data indicating that loss of $p21^{Waf1}$ production is sufficient for normal fibroblasts to bypass senescence (Brown et al., 1997), it seems probable that this reduction in $p21^{Waf1}$ levels is causal in permitting WS cells to bypass M1.

In contrast to HCA2 cells, however, the level of $p16^{Ink4a}$ is reduced in E6-infected WS cells and, although it rises slightly at M^{int}, it is still at a level below that found at M1. This is similar to the changes in $p16^{Ink4a}$ found in IMR90 cells (Dulic et al., 2000). These differences in Cdk inhibitors at M^{int} probably reflect differences between fibroblast strains isolated from different donors and from different tissues. Similarly, although the M^{int} state in WS cells differs from that reported in HCA2 cells (Bond et al., 1999) by the presence of continued cell turnover (with mitotic events being balanced by cell death), it is similar to that reported in other normal cell strains (e.g., IMR90 cells) (Dulic et al., 2000).

We have observed one example of spontaneous escape from M^{int}, in which, ~150 days after entry into M^{int}, a WS.E6 culture began to expand rapidly. After an extended period, this culture underwent a crisis during which the cells died, a situation comparable to that previously reported in normal LF1 cells (Brown et al., 1997). This situation has not been reported for HCA2 cells (Bond et al., 1999); however, Filatov et al. (Filatov et al., 1998) found that E6-infected F5 neonatal foreskin fibroblasts did not proceed to a M^{int}-like state and had few SAβ-gal-producing cells. Instead these cells entered a crisis during which telomerase expression was induced and, thereafter, population expansion was continuous. Ectopic production of hTERT in WS.E6 fibroblasts appears to be equally permissive for continuous expansion.

It remains to speculate about the mechanism of the cell-cycle arrest observed at M^{int} in human fibroblasts. In HCA2 cells, the arrest might be due to the large increase in $p16^{Ink4a}$, because it has been shown that $p16^{Ink4a}$ induction in young and immortalized human fibroblasts can restore growth arrest (McConnell et al., 1998; Vogt et al., 1998). This is unlikely to be the situation in WS cells, because the level of $p16^{Ink4a}$ does not increase. Alternatively, the arrest might be due to the small increase in $p21^{Waf1}$ levels, as has been suggested for IMR90 cells (Dulic et al., 2000). A final possibility is that there is a mechanism that links the erosion of telomeres to cell-cycle arrest that is independent of p53, but whose nature remains obscure (Bond et al., 1999).

Cellular senescence in human fibroblasts appears to be triggered by telomere erosion (Allsop and Harley, 1995; Bodnar et al., 1998; Vaziri and Benchimol, 1998; Wright and Shay, 2002). WS fibroblasts exit the cell cycle at a higher rate than normal fibroblasts and so senesce more rapidly (Faragher et al., 1993), and it appears that their telomeres erode at a greater rate (Schulz et al., 1996), although this is equivocal. Young WS fibroblasts have telomeres of similar length to young normal cells but they senesce with longer mean telomere lengths (Schulz et al., 1996). This might indicate that WS cells are more sensitive to variations in telomere length. However, the telomere length measured by Schulz et al. (Schulz et al., 1996) is a mean length and the presence of a subset of much smaller telomeres in the senescent WS cells is not excluded. More work to resolve this issue is clearly indicated in the future. The longer mean telomere length at senescence might explain the observation that WS.E6 cells make a similar number of PDs as HCA2.E6 cells before the onset of M^{int}, despite the increased rate of erosion. The presence of telomere-driven senescence in WS cells (Ouellette et al., 2000; Wyllie et al., 2000; Choi et al., 2001) and the similarities in the signalling response (this study), would argue for a defect that manifests itself early in the signalling pathway, perhaps by modulating the rate of telomere erosion in WS cells. Thus, a role for WRNp in telomere dynamics is strongly implicated.

The conclusions to be drawn from this work are that WS fibroblasts behave in a way that is similar to normal fibroblasts and that, despite having a much reduced in vitro lifespan, the transducing pathways leading to senescence in WS cells are essentially the same. Thus, the study of premature ageing in WS patients (presumably resulting from this premature replicative senescence) is likely also to reflect the effects of cellular ageing in normal individuals, thus making WS a suitable model for some aspects of the ageing process. This model, in which the loss of WRNp expression is linked to whole body ageing via accelerated replicative senescence, does not exclude other aspects of the WS cellular phenotype contributing to the clinical spectrum of WS; one could readily postulate a link between chromosome instability and the observed increase in mesenchymal cancers in WS (Salk, 1982; Goto et al., 1996). WS is a complex disease and loss of WRNp expression might well contribute to various aspects in different ways.

We thank members of our laboratories for their discussions. This work was supported by the BBSRC's *Science of Ageing* Initiative.

References

Allsopp, R. C. and Harley, C. B. (1995). Evidence for a critical telomere length in senescent human fibroblasts. *Exp. Cell Res*. **219**, 130-136.

Bodnar, A. G., Ouellette, M., Frolkis, M., Holt, S. E., Chiu, C. P., Morin, G. B., Harley, C. B., Shay, J. W., Lichtsteiner, S. and Wright, W. E. (1998). Extension of life-span by introduction of telomerase into normal human cells. *Science* **279**, 349-352.

Bohr, V. A., Souza Pinto, N., Nyaga, S. G., Dianov, G., Kraemer, K., Seidman, M. M. and Brosh, R. M., Jr (2001). DNA repair and mutagenesis in Werner syndrome. *Environ. Mol. Mutagen.* **38**, 227-234.

Bohr, V. A., Brosh, R. M., Jr, von Kobbe, C., Opresko, P. and Karmakar, P. (2002). Pathways defective in the human premature aging disease Werner syndrome. *Biogerontology* **3**, 89-94.

Bond, J. A., Wyllie, F. S. and Wynford-Thomas. D. (1994). Escape from senescence in human diploid fibroblasts induced directly by mutant p53. *Oncogene* **9**, 1885-1889.

Bond, J. A., Blaydes, J. P., Rowson, J., Haughton, M. F., Smith, J. R., Wynford-Thomas, D. and Wyllie, F. S. (1995). Mutant p53 rescues human diploid cells from senescence without inhibiting the induction of SDI1/WAF1. *Cancer Res.* **55**, 2404-2409.

Bond, J., Haughton, M., Blaydes, J., Gire, V., Wynford-Thomas, D. and Wyllie, F. (1996). Evidence that transcriptional activation by p53 plays a direct role in the induction of cellular senescence. *Oncogene* **13**, 2097-2104.

Bond, J. A., Haughton, M. F., Rowson, J. M., Gire, V., Wynford-Thomas, D. and Wyllie, F. S. (1999). Control of replicative life span in human cells: barriers to clonal expansion intermediate between M1 senescence and M2 crisis. *Mol. Cell. Biol*. **19**, 3103-3114.

Böttger, V., Böttger, A., Howard, S. F., Picksley, S. M., Chène, P., Garcia-Echeverria, C., Hochkeppel, H.-K. and Lane, D. P. (1996). Identification of novel mdm2 binding peptides by phage display. *Oncogene* **13**, 2141-2147.

Bringold, F. and Serrano, M. (2000). Tumor suppressors and oncogenes in cellular senescence. *Exp. Gerontol.* **35**, 317-329.

Brown, W. T., Kieras, F. J., Houck, G. E., Jr, Dutkowski, R. and Jenkins,

E. C. (1985). A comparison of adult and childhood progerias: Werner syndrome and Hutchinson-Guildford progeria syndrome. *Adv. Exp. Med. Biol*. **190**, 229-244.

Brown, J. P., Wenyi, W. and Sedivy, J. M. (1997). Bypass of senescence after disruption of p21$^{CIP1/Waf1}$ gene in normal diploid human fibroblasts. *Science* **277**, 831-834.

Choi, D., Whittier, P. S., Oshima, J. and Funk, W. D. (2001). Telomerase expression prevents replicative senescence but does not fully reset mRNA expression patterns in Werner syndrome cell strains. *FASEB. J*. **15**, 1014-1020.

Dimri, G. P., Lee, X., Basile, G., Acosta, M., Scott, G., Roskelley, C., Medrano, E. E., Linskens, M., Rubelj, I., Pereira-Smith, O. et al. (1995). A biomarker that identifies senescent human cells in culture and in aging skin in vivo. *Proc. Natl. Acad. Sci. USA* **92**, 9363-9367.

Dulic, V., Beney, G.-E., Frebourg, G., Drullinger, L. F. and Stein, G. H. (2000). Uncoupling between phenotypic senescence and cell cycle arrest in ageing p21-deficient fibroblasts. *Mol. Cell. Biol.* **20**, 6741-6754.

Epstein, C. J., Martin, G. M., Schultz, A. L. and Motulsky, A. G. (1996). Werner syndrome: a review of its symptomatology, natural history, pathologic features, genetics and relationship to the natural aging process. *Medicine* **45**, 177-221.

Faragher, R. G. A., Kill, I. R., Hunter, J. A., Pope, F. M., Tannock, C. and Shall, S. (1993). The gene responsible for Werner syndrome may be a cell division 'counting' gene. *Proc. Natl. Acad. Sci. USA* **90**, 12030-12034.

Filatov, L., Golubovskaya, V., Hurt, J. C., Byrd, L. L., Phillips, J. M. and Kaufmann, W. K. (1998). Chromosomal instability is correlated with telomere erosion and inactivation of G2 checkpoint function in human fibroblasts expressing human papillomavirus type 16 E6 oncoprotein. *Oncogene* **16**, 1825-1838.

Fukuchi, K., Martin, G. M. and Monnat, R. J., Jr (1989). Mutator phenotype of Werner syndrome is characterised by extensive deletions. *Proc. Natl. Acad. Sci. USA* **86**, 5893-5897.

Gire, V. and Wynford-Thomas, D. (1998). Re-initiation of DNA synthesis and cell division in senescent human fibroblasts by microinjection of anti-p53 antibodies. *Mol. Cell. Biol*. **18**, 1611-1621.

Goto, M., Miller, R. W., Ishikawa, Y. and Sugano, H. (1996). Excess of rare cancers in Werner syndrome (adult progeria). *Cancer Epidemiol. Biomarkers Prev*. **5**, 239-246.

Gray, M. D., Wang, L., Youssoufian, H., Martin, G. M. and Oshima, J. (1998). Werner helicase is localized to transcriptionally active nucleoli of cycling cells. *Exp. Cell. Res*. **242**, 487-494.

Halbert, C. L., Demers, G. W. and Galloway, D. A. (1991). The E7 gene of human papillomavirus type 16 is sufficient for immortalization of human epithelial cells. *J. Virol*. **65**, 473-478.

Hoehn, H., Bryant, E. M., Au, K., Norwood, T. H., Boman, H. and Martin, G. M. (1975). Cytogenetics of Werner's syndrome cultured skin fibroblasts. *Cytogenet. Cell Genet*. **15**, 282-298.

Huang, S., Li, B., Gray, M. D., Oshima, J., Mian, I. S. and Campisi, J. (1998). The premature ageing syndrome protein, WRN, is a 3′→5′ exonuclease. *Nat. Genet.* **20**, 114-116.

Itahana, K., Dimri, G. and Campisi, J. (2001). Regulation of cellular senescence by p53. *Eur. J. Biochem*. **268**, 2784-2791.

Lin, J., Teresky, A. K. and Levine, A. J. (1995). Two critical hydrophobic amino acids in the N-terminal domain of the p53 protein are required for the gain of function phenotypes of human p53 mutants. *Oncogene* **10**, 2387-2390.

Marciniak, R. A., Lombard, D. B., Johnson, F. B. and Guarente, L. (1998). Nucleolar localization of the Werner syndrome protein in human cells. *Proc. Natl. Acad. Sci. USA* **95**, 6887-6892.

Martin, G. M., Sprague, C. C. and Epstein, C. J. (1970). Replicative life span of cultivated human cells. *Lab. Invest*. **23**, 86-92.

Martin, G. M., Oshima, J., Gray, M. D. and Poot, M. (1999). What geriatricians should know about the Werner syndrome. *J. Am. Geriatr. Soc*. **47**, 1136-1144.

McConnell, B. B., Starborg, M., Brookes, S. and Peters, G. (1998). Inhibitors of cyclin-dependent kinases induce features of replicative senescence in early passage human diploid fibroblasts. *Curr. Biol*. **12**, 351-354.

Morgenstern, J. P. and Land, H. (1990). Advanced mammalian gene transfer: high titre retroviral vectors with multiple drug selection markers and a complementary helper-free packaging cell line. *Nucleic Acids Res*. **18**, 3587-3596.

Nakamura, T. M., Morin, G. B., Chapman, K. B., Weinrich, S. L., Andrews, W. H., Lingner, J., Harley, C. B. and Cech, T. R. (1997). Telomerase catalytic subunit homologs from fission yeast and human. *Science* **277**, 955-959.

Ouellette, M. M., McDaniel, L. D., Wright, W. E., Shay, J. W. and Schultz, R. A. (2000). The establishment of telomerase-immortalised cell lines representing human chromosome instability syndromes. *Hum. Mol. Genet*. **9**, 403-411.

Salk, D. (1982). Werner's syndrome: a review of recent research with an analysis of connective tissue metabolism, growth control of cultured cells, and chromosomal aberrations. *Hum. Genet*. **62**, 1-5.

Salk, D., Au, K., Hoehn, H. and Martin, G. M. (1981). Cytogenetics of Werner's syndrome cultured skin fibroblasts: variegated translocation mosaicism. *Cytogenet. Cell Genet.* **30**, 92-107.

Schulz, V. P., Zakian, V. A., Ogburn, C. E., McKay, J., Jarzebowicz, A. A., Edland, S. D. and Martin, G. M. (1996). Accelerated loss of telomere repeats may not explain accelerated replicative decline in Werner syndrome cells. *Hum. Genet.* **97**, 750-754.

Shen, J.-C. and Loeb, L. A. (2001). Unwinding the molecular basis of the Werner syndrome. *Mech. Ageing Dev*. **122**, 921-944.

Sherwood, S. W., Rush, D., Ellsworth, J. L. and Schimke, R. T. (1988). Defining cellular senescence in IMR-90 cells: a flow cytometric analysis. *Proc. Natl. Acad. Sci. USA* **85**, 9086-9090.

Shiratori, M., Sakamoto, S., Suzuki, N., Tokutake, Y., Kawabe, Y., Enomoto, T., Sugimoto, M., Goto, M., Matsumoto, T. and Furuichi, Y. (1999). Detection by epitope-defined monoclonal antibodies of Werner DNA helicases in the nucleoplasm and their upregulation by cell transformation and immortalization. *J. Cell Biol*. **144**, 1-9.

Smith, P. J., Wiltshire, M., Chin, S. F., Rabbitts, P. and Souès, S. (1999). Cell cycle checkpoint evasion and protracted cell cycle arrest in X-irradiated small cell lung carcinoma cells. *Int. J. Radiat. Biol*. **75**, 1137-1147.

Stein, G. H., Beeson, M. and Gordon, L. (1990). Failure to phosphorylate the retinoblastoma gene product in senescent human fibroblasts. *Science* **249**, 666-669.

Stephen, C. W., Helminen, P. and Lane, D. P. (1995). Characterisation of epitopes on human p53 using phage-displayed peptide libraries: insights into antibody-peptide interactions. *J. Mol. Biol*. **248**, 58-78.

Vaziri, H. and Benchimol, S. (1998). Reconstitution of telomerase activity in normal human cells leads to elongation of telomeres and extended reproductive life span. *Curr. Biol*. **8**, 279-282.

Vogt, M. C., Habbblom, J., Yeargin, T., Christiansen-Weber, T. and Haas, M. (1998). Independent induction of senescence by p16^{Ink4a} and p21^{Cip1} in spontaneously immortalised human fibroblasts. *Cell Growth Differ*. **9**, 139-146.

Webley, K., Bond, J. A., Jones, C. J., Blaydes, J. P., Craig, A., Hupp, T. and Wynford-Thomas, D. (2000). Posttranslational modifications of p53 in replicative senescence overlapping but distinct from those induced by DNA damage. *Mol. Cell. Biol*. **20**, 2803-2808.

Wright, W. E. and Shay, J. W. (2002). Historical claims and current interpretations of replicative aging. *Nat. Biotechnol*. **20**, 682-688.

Wyllie, F., Lemoine, N., Barton, C., Dawson, T., Bond, J. and Wynford-Thomas. D. (1993). Direct growth stimulation of normal human epithelial cells by mutant p53. *Mol. Carcinogen*. **7**, 83-88.

Wyllie, F. S., Jones, C. J., Skinner, J. W., Haughton, M. F., Wallis, C., Wynford-Thomas, D., Faragher, R. G. A. and Kipling, D. (2000). Telomerase prevents the accelerated ageing of Werner syndrome fibroblasts. *Nat. Genet*. **24**, 16-17.

Yu, C. E., Oshima, J., Fu, Y. H., Wijsman, E. M., Hisama, F., Alisch, R., Matthews, S., Nakura, J., Miki, T., Ouais, S. et al. (1996). Positional cloning of the Werner's syndrome gene. *Science* **272**, 258-262.